Geophysical Journal (1988) **94**, 575–580

RESEARCH NOTE

Ray tracing in anisotropic media with a linear gradient

P. M. Shearer* and C. H. Chapman†

Bullard Laboratories, Department of Earth Sciences, University of Cambridge, Madingley Rise, Madingley Road, Cambridge CB3 0EZ, *UK*

Accepted 1988 March 25. Received 1988 March 22; in original form 1988 January 15

SUMMARY

In general, ray paths in anisotropic media can be found by solving the sixth-order kinematic ray equations. In this paper it is shown that in media where the density-normalized elastic parameters depend quadratically on one coordinate, i.e. the velocities vary linearly, the projection of the ray path on to the slowness vector plane, which is fixed, is the same shape as the cross-section of the slowness surface. Thus the ray path can be found by solving a polynomial equation. The deviation of the ray path from the plane and the travel time can be calculated by evaluating a simple integral along the ray.

Key words: anisotropic media, linear velocity, ray tracing

INTRODUCTION

The study of wave propagation in anisotropic media is attracting much attention (e.g. November 1987 issue of this journal). Although the fundamental theory is well understood (e.g. Crampin 1981; Fryer & Frazer 1984), it remains a significant task to compute synthetic seismograms in realistic anisotropic media. As in isotropic media, an attractive approximation is to use asymptotic ray theory. Again the fundamental theory is well understood (Červený 1972), but the ray equations are sufficiently complicated that computations are expensive. In isotropic media the situation is considerably simpler. Although the differential ray equations are of the same order, the elements in the equations are much simpler and easier to compute. More importantly, the ray equations need not be solved numerically as several analytic solutions exist (Červený 1987). Numerical solutions are only needed when interpolation methods are used for which no analytic solution is known. An example is the use of cubic splines to avoid velocity or gradient discontinuities (SEIS83–Červený 1985a). Normally these higher-order interpolation methods are used to obtain smooth travel-time curves to simplify two point ray tracing and the application of geometrical ray theory. Our knowledge of the model structure does not require or justify the use of a high-order interpolation method. It is merely required to avoid or reduce the singularities of geometrical ray theory. Recent extensions of geometrical ray theory for the computation of synthetic seismograms, e.g. the Gaussian beam method (Červený 1985b) and Maslov asymptotic theory (Chapman & Drummond 1982), circumvent these problems by band-limiting and smoothing the seismograms. For these purposes it is no longer necessary to ray-trace through smooth models and simple interpolation methods can be used.

The simplest method of interpolation is to divide the model into homogeneous elements so that all ray segments are straight. However, the discontinuities in velocities may cause significant problems as rays can be totally reflected, producing notable discontinuities in the travel-time curves. A popular alternative is to interpolate the velocity linearly (Will 1976; Whittal & Clowes 1979; Marks & Hron 1980). If the model is divided into elements of tetrahedra, laterally homogeneous layers, etc., the linear velocity function is uniquely defined in each element and continuous between elements. In this paper we only consider ray tracing through a single model element in which a linear velocity function is assumed. As in isotropic models, laterally inhomogeneous structures can be modelled by combining many such elements. Within the element, we refer to the velocity as varying in the 'vertical' direction and the element as being 'horizontally' homogeneous. These terms are used for convenience and, in general laterally heterogeneous models, the velocity gradient in each element can be in a different direction which differs from the true vertical.

In isotropic media, ray paths in a linear velocity function are arcs of circles. Thus ray tracing is simplified as the simple geometry allows rays to be solved across each element in a single step without finding intermediate points, however large the element. In this paper we investigate the same problem in anisotropic media. As the velocities depend only on the 'vertical' coordinate, the 'horizontal' components of the slowness vector perpendicular to this direction are constant. Thus the slowness vector remains within a fixed plane defined by the 'vertical' direction and the fixed 'horizontal' slowness direction. In the next section we show that the projection of the ray path on to this plane

* Now at: Institute of Geophysics and Planetary Physics, Scripps Institution of Oceanography, U.C. San Diego, CA 92093.
† Now at: Department of Physics, University of Toronto, Toronto, Ontario M5S 1A7, Canada.

is the same shape as the cross-section of the slowness surface. Bennett (1968) obtained a similar result for transversely isotropic media. In isotropic media, the slowness surface is a sphere and the cross-section a circle, as expected. Thus two coordinates of the ray path can be found by solving a polynomial for the slowness surface. Examples are given for some interesting anisotropic media in the third section of this paper. The third coordinate, the deviation of the ray path from the slowness plane, can be calculated by evaluating a simple integral along the ray, as can the travel time.

THEORY

The theory of ray tracing in inhomogeneous, anisotropic media is well known (Červený 1972). We follow the standard notation and only quote the results we need. A slowness surface (e.g. Fig. 1a) in an anisotropic medium is defined by the equation

$$G(\mathbf{x}, \mathbf{p}) = 1 \tag{1}$$

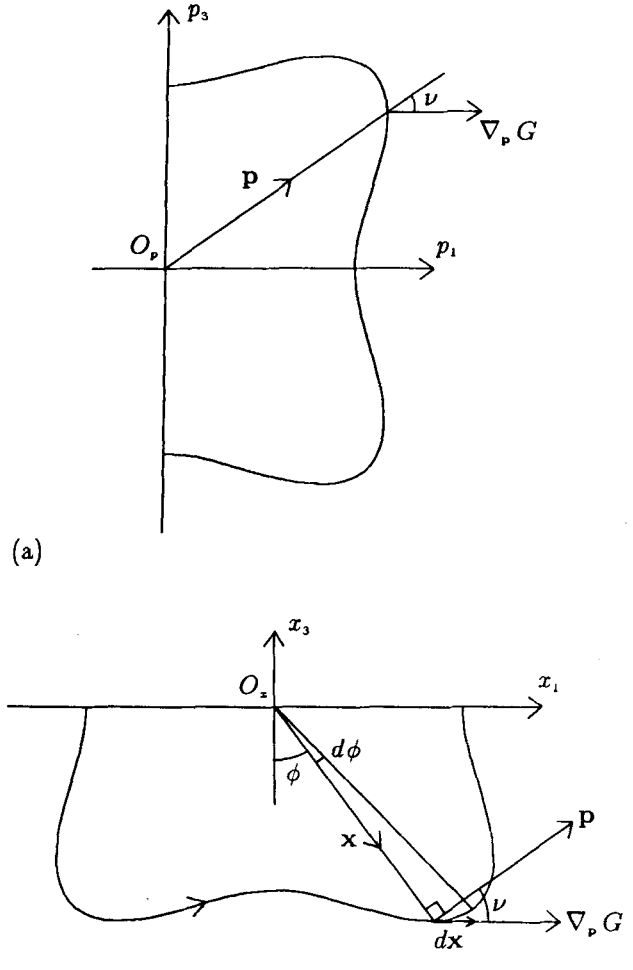

Figure 1. (a) The slowness surface defined by $G(\mathbf{x}, \mathbf{p}) = 1$ with $p_2 = 0$. The normal to the slowness surface, $\nabla_p G$, makes an angle ν with the slowness vector $\mathbf{p}$. (b) The ray path projected onto the x_1–x_3 plane. The position vector $\mathbf{x}$ makes an angle ϕ with the x_3-axis, the slowness vector $\mathbf{p}$ is perpendicular to $\mathbf{x}$, and the ray segment, $d\mathbf{x}$, is in the direction of $\nabla_p G$.

where G is an eigenvalue of the characteristic equation

$$|\Gamma_{jk} - G\delta_{jk}| = 0. \tag{2}$$

In these equations Γ_{jk} is an element of the Christoffel matrix, $\Gamma_{jk} = p_i p_l a_{ijkl}$. The density-normalized elastic parameters are $a_{ijkl} = c_{ijkl}/\rho$ where c_{ijkl} are the anisotropic elastic parameters, and $p_i = \partial\tau/\partial x_i$ are the components of the slowness vectors. The travel time is τ and density is ρ.

The partial differential equation (1) can be solved by the method of characteristics to give the kinematic ray equations:

$$\begin{aligned} (dx_i/d\tau) &= \tfrac{1}{2}(\partial G/\partial p_i), \\ (dp_i/d\tau) &= -\tfrac{1}{2}(\partial G/\partial x_i). \end{aligned} \tag{3}$$

We now consider the special case where the 'velocity gradient' is constant. A linear velocity function is commonly used in isotropic models as it is a simple method of interpolation and results in circular ray paths. Without loss in generality we can rotate the coordinate system so that the elastic parameters are functions of one coordinate, x_3, only. Again without loss in generality, we can translate this coordinate so its origin coincides with the zero-velocity plane (obviously not part of the physical model but obtained by extrapolation of the linear velocity). We later assume that x_3 is chosen so that the model exists for $x_3 < 0$, e.g. Fig. 1(b). We assume that these coordinate transformations have been applied and the above equations are written with respect to these coordinates. Thus the density-normalized elastic parameters can be written

$$a_{ijkl}(\mathbf{x}) = A_{ijkl} x_3^2. \tag{4}$$

As the elastic parameters are only a function of x_3, the slowness surface equation (1) is independent of x_1 and x_2. Thus the ray equations (3) give

$$(dp_1/d\tau) = (dp_2/d\tau) = 0 \tag{5}$$

and p_1 and p_2 are constant along the ray, the well known conservation of 'horizontal' slowness (calling x_3 the 'vertical' coordinate). Again, without loss in generality, we can rotate the coordinate system about the 'vertical' x_3-axis so $p_2 = 0$. We assume that this transformation has also been applied to the above equations. Note that this coordinate transformation does not imply that x_2 is zero, as in anisotropic media the slowness vector is not the same as the ray direction.

With these three transformations, the equation for the slowness surface (1) can be reduced to

$$G(x_3, p_1, p_3) = 1. \tag{6}$$

As G is a homogeneous function of second order in p_i, Euler's theorem gives (Červený 1972)

$$p_i(\partial G/\partial p_i) = 2G.$$

Combining with the ray equations (3) and $G = 1$, we obtain

$$p_i(dx_i/d\tau) = 1. \tag{7}$$

For the linear velocity behaviour, G is quadratic in x_3 so, similarly,

$$x_3(\partial G/\partial x_3) = 2G,$$

and again combining with the ray equations (3), (5) and

$G = 1$, we have

$$x_i(dp_i/d\tau) = -1. \tag{8}$$

Combining equations (7) and (8), we obtain

$$(d/d\tau)(\mathbf{x} \cdot \mathbf{p}) = 0.$$

The origin of $\mathbf{x}$ is restricted to the plane $x_3 = 0$, but can be translated anywhere in this plane. For some initial point on the ray, we chose the x_1 origin so $\mathbf{x}$ and $\mathbf{p}$ are perpendicular, and then obtain the result

$$\mathbf{x} \cdot \mathbf{p} = 0 \tag{9}$$

everywhere on the ray (Fig. 1b). The x_2 origin is arbitrary and can be chosen so $x_2 = 0$ at an initial point on the ray.

The slowness surface (6) scales inversely with the x_3-coordinate. Thus if we choose to fix this coordinate at some arbitrary value, $x_3 = X_3$, a constant, we can obtain the slowness surface at any 'depth' from

$$G\left(X_3, \frac{x_3}{X_3}p_1, \frac{x_3}{X_3}p_3\right) = 1. \tag{10}$$

Using result (9), this can be rewritten

$$G\left(X_3, \frac{p_1}{X_3}x_3, -\frac{p_1}{X_3}x_1\right) = 1. \tag{11}$$

For fixed x_3, e.g. X_3, equation (10) connects p_1 and p_3, and defines the slowness surface. From equation (5), p_1 is fixed along a ray, and thus equation (11) connects x_1 and x_3, and defines the ray path (in the x_1–x_3 plane). But the function G is the same in both cases, and so the ray path can be obtained by rotating the slowness surface through 90° (so the p_3-axis corresponds to the x_1-axis, and the p_1-axis to minus the x_3-axis) and scaling appropriately, i.e. the slowness values for the surface at $x_3 = X_3$ are multiplied by $|X_3/p_1|$ (remember in (11) that X_3 is negative). A similar result was obtained by Bennett (1968) for the special case of transversely isotropic material.

Equation (11) for the ray path does not imply that $x_2 = 0$, only that the projection of the ray path onto the x_1–x_3 plane is similar to the slowness curve. The transverse horizontal coordinate, x_2, is undetermined by this equation. It can be determined by integrating the appropriate ray equation (3),

$$x_2 = \tfrac{1}{2}\int \frac{\partial G}{\partial p_2}\, d\tau. \tag{12}$$

On symmetry planes the integrand is zero and the ray does not deviate from the plane. We return below to a discussion of evaluating integral (12) in general.

In order to evaluate the travel time, we consider equation (7). The slowness vector can be written as

$$\mathbf{p} = \left(p_1, 0, -\frac{x_1}{x_3}p_1\right) \tag{13}$$

to satisfy (9). Thus from (7) we obtain

$$d\tau = p_1\, dx_1 + p_3\, dx_3$$

$$= \frac{p_1}{x_3}|\mathbf{x} \times d\mathbf{x}|$$

$$= \frac{p_1}{x_3}|\mathbf{x}|^2\, d\phi,$$

where $d\phi$ is the angle subtended at the origin by the ray segment $d\mathbf{x}$ (Fig. 1b). Thus

$$d\tau = p_1\, |\mathbf{x}| \sec\phi\, d\phi \tag{14}$$

where ϕ is the angle between $\mathbf{x}$ and the x_3-axis. The travel time between two points can be obtained from

$$\tau = p_1 \int_{\chi_2}^{\chi_1} |\mathbf{x}|\, d\chi, \tag{15}$$

where $\chi = \tanh^{-1}(\sin\phi)$ (so $d\chi = \sec\phi\, d\phi$). We have written the result in this form as in isotropic media $|\mathbf{x}|$ is constant (the radius of the circular ray) and

$$\tau = p_1\, |\mathbf{x}|\, (\chi_2 - \chi_1),$$

the well known travel-time result for a linear velocity function (Gebrande 1976) with $p_1\, |\mathbf{x}| = 1/|\nabla v|$. In anisotropic media, $|\mathbf{x}|$ will vary slowly and the integral (15) is easily evaluated.

It is easily shown that expression (14) is equivalent to distance divided by velocity. It is well known that the ratio of the normal (phase) velocity V and the ray (group) velocity v gives the cosine of the angle between the ray and the normal to the wavefront (Červený 1972), i.e.

$$\cos\nu = (V/v),$$

where ν is illustrated in Fig. 1. Thus

$$|d\mathbf{x}| = |\mathbf{x}|\, d\phi \sec\nu$$

$$= v\, |\mathbf{x}|\, d\phi/V,$$

but

$$p_1 \sec\phi = |\mathbf{p}| = V^{-1},$$

so

$$d\tau = |d\mathbf{x}|/v$$

as required.

The integral (12) can be converted into an integral with respect to ϕ (or χ) using (14). The partial derivative of G can be obtained without differentiation in the standard manner, i.e.

$$\tfrac{1}{2}(\partial G/\partial p_2) = a_{2jkl}p_l D_{jk}/D,$$

where we have used the usual notation for the Ds (Červený 1972). In this expression p_1 is constant, $p_2 = 0$ and $p_3 = p_1 \tan\phi$. Straightforward but algebraically complicated expressions can therefore be obtained for $\partial G/\partial p_2$ in terms of ϕ. The evaluation of the integrals (12) and (15) is simple compared with the ray equations (3) as the ray path is known independently.

EXAMPLES

As an example, we calculated ray paths for an anisotropic model of aligned cracks in the uppermost crust. We used the theoretical model of Hudson (1980) to determine the elastic constants of a host rock ($\alpha = 4.5\ \mathrm{km\,s^{-1}}$, $\beta = 2.53\ \mathrm{km\,s^{-1}}$, $\rho = 2.8\ \mathrm{Mg\,m^{-3}}$) containing aligned, water-filled cracks with aspect ratio $d = 0.001$ and crack density $\epsilon = 0.1$. The resulting density-normalized elastic constants are: $a_{1111} = 20.04$, $a_{2222} = 20.22$, $a_{1212} = 5.10$, $a_{2323} = 6.38$, $a_{1122} = 7.41\ \mathrm{km^2\,s^{-2}}$, with a (100) hexagonal symmetry axis. This model is then rotated 30° about the (010) axis for the first

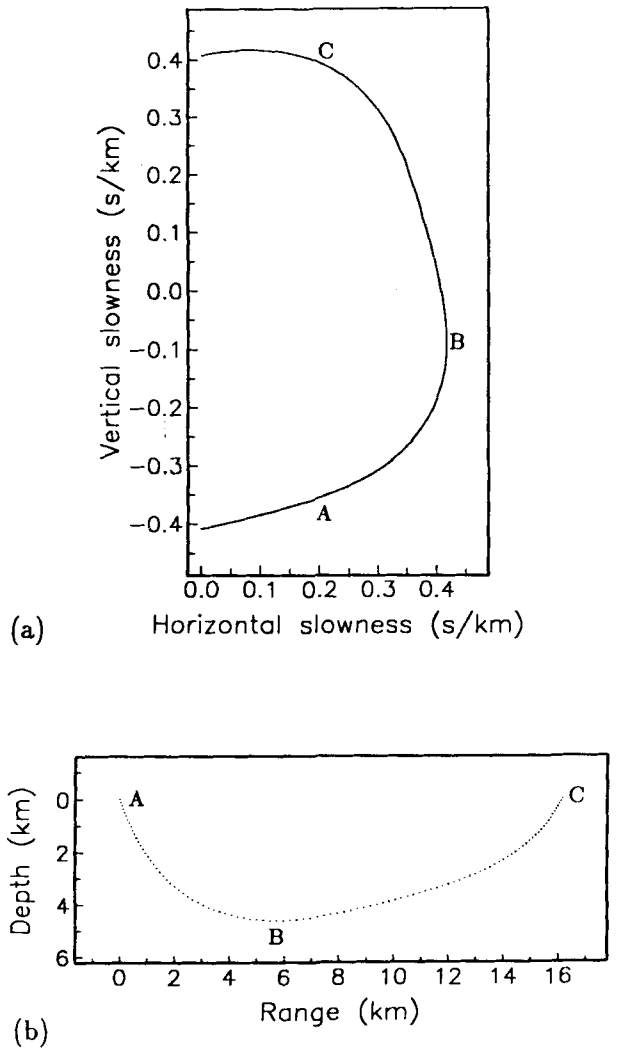

Figure 2. (a) Slowness sheet cross-section. (b) Corresponding ray path for an aligned crack model of anisotropy with a vertical velocity gradient. Points are shown every 0.05 s along the ray path.

example (Fig. 2), and rotated 30° about the (001) axis for the second example (Fig. 3). We assume that a_{ijkl} varies with x_3 according to (4), and that the above values apply at zero depth corresponding to the reference coordinate, X_3. Thus the depth is $(X_3 - x_3)$ and in the examples we take $X_3 = -4.405$ km. For qP-waves, the resulting velocity gradient is about $1.0\,\mathrm{s}^{-1}$.

In Fig. 2(a), we show a cross-section (in the $p_1 - p_3$ plane) of the qSP-wave slowness sheet for the aligned crack model at zero depth, where following the notation of Crampin (1981), qSP is defined as the quasi-shear wave with polarization within a symmetry plane of the anisotropy. The model has been rotated by 30° so that the symmetry axis dips 30° from the horizontal (appropriate if the aligned cracks dip 60°). Because of this rotation, the slowness sheet is not symmetric about the horizontal p_1-axis. Fig. 2(b) shows a qSP-wave ray path for this model, assuming a horizontal slowness $p_1 = 0.2037\,\mathrm{s\,km}^{-1}$. The ray path was calculated using the kinematic ray equations (3); points are shown every 0.05 s along the ray path. As expected, the shape of the ray path is the same as the shape of the corresponding slowness sheet rotated by 90°. The curves shown in Fig. 2 have been scaled such that they are the same size; this scaling was obtained by multiplying the slowness values by $|X_3/p_1|$. Points A, B and C show corresponding points on the slowness surface (Fig. 2a) and ray path (Fig. 2b). The turning point (B) does not correspond to zero vertical slowness, but to the point at which the normal to the slowness surface is horizontal. The travel time of 5.10 s between points A and C can be calculated either from the kinematic ray equations (3) or by the integral (15).

In this example, the cross-section shown in Fig. 2(a) is a symmetry plane in the anisotropy, so the normal to the

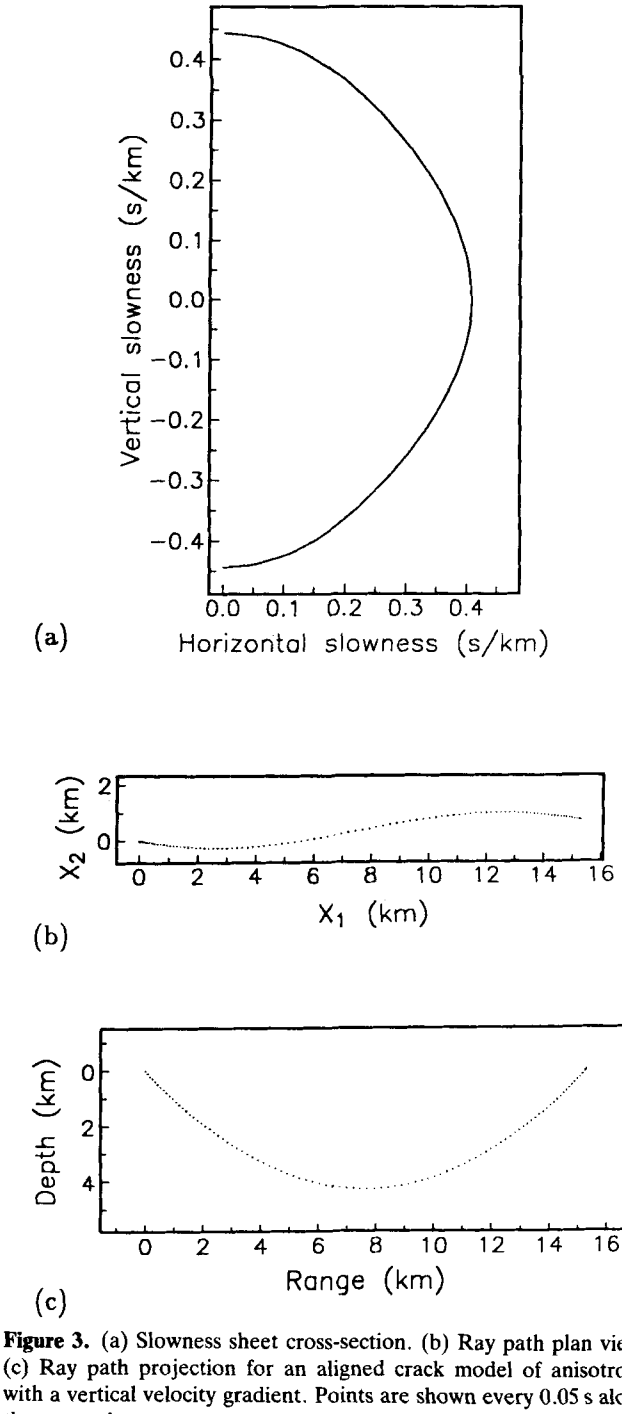

Figure 3. (a) Slowness sheet cross-section. (b) Ray path plan view. (c) Ray path projection for an aligned crack model of anisotropy with a vertical velocity gradient. Points are shown every 0.05 s along the ray path.

slowness surface is within this plane, and the corresponding ray path is also confined to this plane. More generally, the ray path will not be confined to a plane. This is illustrated in Fig. 3(a), which shows a cross-section (in the p_1–p_3 plane) of the *qSP*-wave slowness sheet for the aligned crack model at zero depth. The model has been rotated 30° about the (001) axis, so that the symmetry axis is not within the plane of the cross-section. Normals to the slowness surface (the ray directions) deviate from this plane, and thus the corresponding ray path is not confined to the plane. This is illustrated in Figs 3(b) and 3(c), which show a ray path for this model, calculated from the kinematic ray equations assuming a horizontal slowness $p_1 = 0.2070\,\mathrm{s\,km^{-1}}$. Points are shown every 0.05 s along the ray path. The plan view (Fig. 3b) illustrates how the ray path bends out of the x_1–x_3 plane. This ray path deviation was discussed by Crampin *et al.* (1982) and Shearer & Orcutt (1985). However, the projection of the ray path into the x_1–x_3 plane (Fig. 3c) is exactly the same shape as the slowness curve (Fig. 3a). The

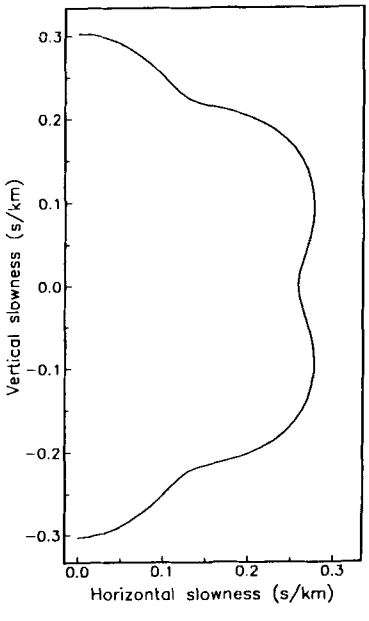

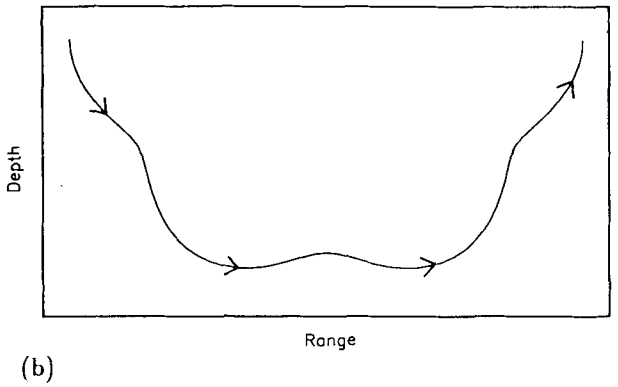

Figure 4. (a) Slowness sheet cross-section. (b) Corresponding ray path for an anisotropic model with a vertical velocity gradient, based on the elastic constants for α-quartz.

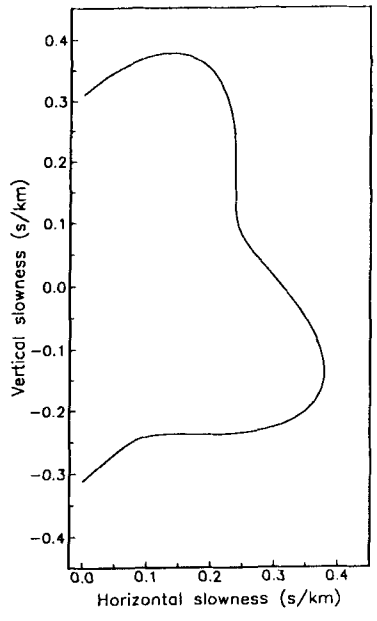

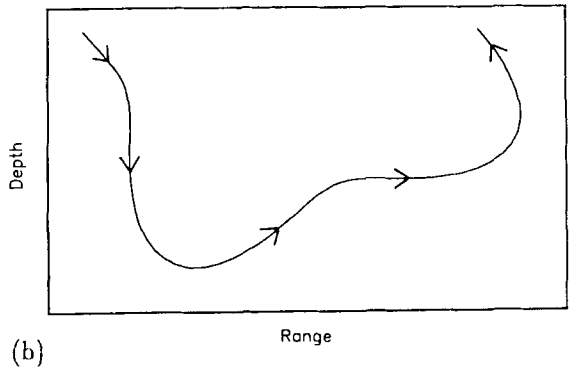

Figure 5. As in Fig. 4, but for iron.

x_2 component of the ray can be obtained from integral (12), while the travel time can be obtained from integral (15).

When the anisotropy is strong, such that sections of the slowness surface are concave outward, the resulting ray paths can appear somewhat peculiar. This is illustrated in Figs 4 and 5, which show slowness sheets and corresponding ray paths for two extreme anisotropy models. Fig. 4(a) shows a cross-section (in the p_1–p_3 plane) of a *qS*-wave slowness sheet for α-quartz. α-quartz has trigonal symmetry with density-normalized elastic constants of $a_{1111} = 32.73$, $a_{3333} = 40.45$, $a_{1122} = 2.64$, $a_{1133} = 4.49$, $a_{2323} = 21.86$, $a_{1123} = -6.76\,\mathrm{km^2\,s^{-2}}$ (Bechmann 1958). For this example, we have rotated the anisotropy by 90° about the (010) axis. Figure 4(b) is simply a 90° rotation of Fig. 4(a) and shows the corresponding ray path if a linear vertical velocity gradient (4) is assumed in the material. The scale on Fig. 4(b) is not shown, since it will depend upon p_1 and X_3. In

this case, the ray has three different turning points, i.e. two concave upward turning points separated by a concave downward turning point.

Figure 5(a) shows a cross-section (in the p_1–p_3 plane) of a qS-wave slowness sheet for iron. Iron has cubic symmetry with density-normalized elastic constants of $a_{1111} = 29.64$, $a_{1122} = 17.71$, $a_{2323} = 14.78\,\mathrm{km^2\,s^{-2}}$ (Musgrave 1970). For this example, we have rotated the anisotropy 20° about the (010) axis. If a vertical velocity gradient is assumed in the material the resulting ray path will correspond to Fig. 5(b). In this case, the ray points backwards (i.e. opposite to its eventual destination) near one of the surface points, and there are relatively straight sections along the ray path where the ray travels vertically or horizontally. The sharp bends in the ray paths in Figs 4(b) and 5(b) would be diagnostic of lateral heterogeneity in isotropic media. However, in these examples the material is laterally homogeneous, and the bends in the ray paths arise purely from the depth-dependence of the anisotropy.

CONCLUSIONS

The equivalence between slowness curves and ray paths provides a relatively efficient way of calculating ray paths through gradient regions. Points on the ray path are constructed by solving the polynomial (1) for **p** with fixed **x**, and scaling appropriately. Each point is obtained directly without requiring the solution for previous points, whereas the kinematic ray equations must be solved for a sequence of points along the ray. This is an advantage in solving two-point ray tracing problems etc., since intermediate points along the ray path need not be found until the correct ray is known and the travel time is calculated. In addition, the numerical instabilities associated with ray tracing near or through singularities on the quasi-shear-wave slowness sheets are completely avoided as the ray paths are constructed geometrically. The main limitation of this technique is that it does not provide a way of ray tracing through regions which contain a gradient between different types of anisotropy. For example, it is not applicable to a region where the anisotropy orientation rotates smoothly with depth (such as the 'anvil' model of the lithosphere beneath southern Germany proposed by Fuchs 1983), or where anisotropy grades smoothly into isotropy (such as the model for the upper oceanic crust proposed by Stephen 1985). In these cases the kinematic ray-tracing equations must be used. However, if significant portions of anisotropic models can be approximated as linear gradients, then a general anisotropic ray tracing code could be made more efficient by using the relationships discussed here.

ACKNOWLEDGMENT

This research was partially supported by Shell UK Exploration and Production, Department of Earth Sciences publication no. 1189.

REFERENCES

Bechmann, R., 1958. Elastic and piezoelectric constants of alpha-quartz, *Phys. Rev.*, **110,** 1060–1061.

Bennett, H. F., 1968. An investigation into velocity anisotropy through measurements of ultrasonic wave velocities in snow and ice cores from Greenland and Antarctica, *PhD thesis,* University of Wisconsin.

Červený, V., 1972. Seismic rays and ray intensities in inhomogeneous anisotropic media, *Geophys. J. R. astr. Soc.*, **29,** 1–13.

Červený, V., 1985a. Ray synthetic seismograms for complex two-dimensional and three-dimensional structures, *J. Geophys.*, **58,** 2–26.

Červený, V., 1985b. Gaussian beam synthetic seismograms, *J. Geophys,* **58,** 44–72.

Červený, V., 1987. Ray tracing algorithms in three-dimensional laterally varying layered structures, in *Seismic Tomography,* pp. 99–133, ed. Nolet, G. D., Reidel, Dordrecht.

Chapman, C. H. & Drummond, R., 1982. Body-wave seismograms in inhomogeneous media using Maslov asymptotic theory, *Bull. seism. Soc. Am.*, **72,** S277–S317.

Crampin, S., 1981. A review of wave motion in anisotropic and cracked elastic-media, *Wave Motion,* **3,** 343–391.

Crampin, S., Stephen, R. A. & McGonigle, R., 1982. The polarization of *P*-waves in anisotropic media, *Geophys. J. R. astr. Soc.*, **68,** 477–485.

Fryer, G. J. & Frazer, L. N., 1984. Seismic waves in stratified anisotropic media, *Geophys. J. R. astr. Soc.*, **78,** 691–710.

Fuchs, K., 1983. Recently formed elastic anisotropy and petrological models for the continental subcrustal lithosphere in southern Germany, *Phys. Earth planet. Int.*, **31,** 93–118.

Gebrande, H., 1976. A seismic-ray tracing method for two-dimensional inhomogeneous media, in *Explosion seismology in Central Europe: Data and Results,* pp. 162–167, eds Giese, P., Prodehl, C. & Stein, A., Springer, Berlin.

Hudson, J. A., 1980. Overall properties of a cracked solid, *Math. Proc. Camb. phil. Soc.*, **88,** 371–384.

Marks, L. W. & Hron, F., 1980. Calculation of synthetic seismograms in laterally inhomogeneous media, *Geophysics,* **45,** 509–510.

Musgrave, M. J. P., 1970. *Crystal Acoustics,* Holden-Day, London.

Shearer, P. M. & Orcutt, J. A., 1985. Anisotropy in the oceanic lithosphere – theory and observations from the Ngendei seismic refraction experiment in the southwest Pacific, *Geophys. J. R. astr. Soc.*, **80,** 493–526.

Stephen, R. A., 1985. Seismic anisotropy in the upper oceanic crust, *J. geophys. Res.*, **90,** 11383–11396.

Whittal, K. P. & Clowes, R. M., 1979. A simple, efficient method for the calculation of travel-times and ray paths in laterally inhomogeneous media, *J. Can. Soc. Exp. Geophys.*, **15,** 21–29.

Will, M., 1976. Calculation of travel-times and ray paths for lateral inhomogeneous media, in *Explosion Seismology in Central Europe: Data and Results,* pp. 168–177, eds Giese, P., Prodehl, C. & Stein, A., Springer, Belin.